Macrophages are primed to transdifferentiate into fibroblasts in malignant ascites and pleural effusions

伊東, 守

Cancer Letters 532 (2022) 215597

Contents lists available at ScienceDirect

Cancer Letters

journal homepage: www.elsevier.com/locate/canlet

Original Articles

Macrophages are primed to transdifferentiate into fibroblasts in malignant ascites and pleural effusions

Mamoru Ito [a], Michitaka Nakano [a], Hiroshi Ariyama [a], Kyoko Yamaguchi [a], Risa Tanaka [b], Yuichiro Semba [a], Takeshi Sugio [a], Kohta Miyawaki [a], Yoshikane Kikushige [a], Shinichi Mizuno [a], Taichi Isobe [c], Kenro Tanoue [a], Ryosuke Taguchi [a], Shohei Ueno [a], Takahito Kawano [d], Masaharu Murata [d], Eishi Baba [c,*], Koichi Akashi [a]

[a] Department of Medicine and Biosystemic Science, Kyushu University Graduate School of Medical Sciences, Fukuoka, Japan
[b] Department of Medical Oncology, Hamanomachi Hospital, Fukuoka, Japan
[c] Department of Oncology and Social Medicine, Faculty of Medical Sciences, Kyushu University, Fukuoka, Japan
[d] Center for Advanced Medical Innovation, Kyushu University, Fukuoka, Japan

ARTICLE INFO

Keywords:
Tumor-associated macrophage
Cancer-associated fibroblast
Tumor microenvironment

ABSTRACT

Cancer-associated fibroblasts (CAFs) play an important role in cancer progression. However, the origin of CAFs remains unclear. This study shows that macrophages in malignant ascites and pleural effusions (cavity fluid-associated macrophages: CAMs) transdifferentiate into fibroblast-like cells. CAMs obtained from gastrointestinal cancer patients were sorted by flow cytometry and cultured in vitro. $CD45^{+}CD14^{+}$ CAMs transdifferentiated into $CD45^{-}CD90^{+}$ fibroblast-like cells that exhibited spindle shapes. Then, cDNA microarray analysis showed that the $CD45^{-}CD90^{+}$ fibroblast-like cells (macrophage-derived CAFs: MDCAFs) had a fibroblast-specific gene expression signature and produced growth factors for epithelial cell proliferation. Human colon cancer cells transplanted into immunodeficient mice with MDCAFs formed larger tumors than cancer cells alone. Gene ontology analyses showed the involvement of TGFβ signaling and cell-matrix adhesion in MDCAFs, and transdifferentiation of CAMs into MDCAFs was canceled by inhibiting TGFβ and cell adhesion. Furthermore, the acquired genetic alterations in hematopoietic stem cells (HSCs) were shared in CAMs and MDCAFs. Taken together, CAMs could be a source of CAFs and might originate from HSCs. We propose the transdifferentiation process of CAMs into MDCAFs as a new therapeutic target for fibrosis associated with gastrointestinal cancer.

1. Introduction

Various non-cancerous cells are involved in the cancer progression process and act as a "tumor microenvironment" [1]. Of these cells, tumor-associated macrophages (TAMs) and cancer-associated fibroblasts (CAFs) play important roles in the tumor microenvironment. Macrophages have phenotypical heterogeneity and change the cell state with organ and microenvironment. Historically, macrophage subtypes are broadly categorized into two cell types, classically activated pro-inflammatory macrophages (here simply describe as "M1 macropahges") and alternatively activated macrophages (simplified as "M2 macrophages"). TAMs are generally polarized to M2 phenotype in various types of cancer [2]. M2 macrophages suppress inflammation and promote tissue repair processes to maintain homeostasis. However, these processes also benefit tumor expansion. M2-like TAMs suppress tumor immunity by producing anti-inflammatory cytokines such as IL-10 and TGFβ. They also contribute to tumor cell proliferation by producing several growth factors, including basic FGF, HGF, EGF, and PDGF [3].

CAFs also have various roles in cancer. They promote tumor cell proliferation, extracellular matrix remodeling, immune modulation, and angiogenesis via their secretome [4,5]. The origin of CAFs is not considered uniform, and several cells have been reported as the source, such as residential fibroblasts, endothelial cells, and circulating mesenchymal stem cells [4].

Abundant macrophages and fibroblasts reside in ascites, mesentery,

Abbreviations: cavity fluid-associated macrophages, CAMs; macrophage-derived CAFs, MDCAFs.

* Corresponding author. Department of Oncology and Social Medicine, Graduate School of Medical Sciences, Kyushu University, Fukuoka, 812, Japan.
E-mail address: baba.eishi.889@m.kyushu-u.ac.jp (E. Baba).

https://doi.org/10.1016/j.canlet.2022.215597
Received 19 May 2021; Received in revised form 2 February 2022; Accepted 8 February 2022
Available online 10 February 2022

and the omentum of patients with malignant ascites [6,7]. They also act as TAMs and CAFs, contributing to tumor progression. Proliferation of CAFs causes fibrosis of the mesentery and omentum, resulting in bowel dysfunction and finally leading to bowel obstruction [8]. From the recent findings described above, TAMs and CAFs in patients with malignant ascites are thought to have crucial roles in the process of the spread of tumor cells in the peritoneal cavity.

Desmoplastic, stromal lesions of cancer are generally accompanied by macrophage infiltration [9]. It is largely believed that TAMs contribute indirectly to the proliferation of CAFs because TAMs are reported to produce profibrotic mediators and promote fibroblast activation [10]. On the other hand, there is accumulating evidence confirming that macrophages are able to acquire fibroblast progenitor properties in the field of fibrotic disease research [11–13]. Interestingly, CAFs share their secretome with TAMs, including basic FGF, HGF, EGF, PFGF, IL-6, and TGFβ [4,5]. However, whether macrophages are able to acquire fibroblastic features in the tumor microenvironment remains unclear. This study proves that macrophages in cavity fluid (ascites and pleural effusion) directly transdifferentiate into fibroblast-like cells and promote tumor progression, as well as CAFs. Inhibiting this transdifferentiation process may bring a new strategy for preventing tumor dissemination in the peritoneal cavity.

2. Materials and methods

2.1. Patients' samples

Samples of ascites or pleural effusion due to tumor dissemination of digestive organ cancers were obtained from 5 institutions from July 2014 to December 2021. All human samples were collected with written, informed consent. This study was performed after approval by the institutional review board of each institution.

2.2. Cell lines

DLD-1 was obtained from American Type Culture Collection. NUGC-4 was from JCRB Cell Bank. KMOA103 was established from malignant ascites due to pancreatic carcinoma in Kyushu University Hospital. Cells were cultured in RPMI medium (RPMI-1640, Wako) supplemented with 10% (v/v) fetal bovine serum (FBS) (Sigma-Aldrich) and penicillin streptomycin (Penstrep, Thermo Fisher Scientific). Lentivirus particles were harvested 72 h after pLenti-PGK-Venus-Akaluc (Addgene Plasmid #124701) transfection with the packaging plasmid psPAX2 and VSV-G envelope plasmid into HEK293T cells by using polyethylenimine (PEI). DLD-1 cells were transduced with lentiviral particles and selected 48–72h after by using FACS method (BD FACSAria™III), sorting Venus + cells.

2.3. Cell separation and cell culture

The collected fluid samples were centrifuged immediately after being drained from patients and the cell fraction and supernatant were separated. Red blood cells in the cell fraction were lysed with BD Pharm Lyse (BD Bioscience). Cells were analyzed or cultured after passage through a 70-μm filter (BD Bioscience). The collected cells were cultured with Macrophage SFM (Thermo Fisher Scientific) containing 1% penicillin/streptomycin. FBS, 10 ng/mL TGFbeta1 (Peprotech), and 10 μM SB431542 (Wako) were added according to each experimental condition. The images of cultured cells were acquired by phase-contrast microscopy (KEYENCE BZ-X700). KEYENCE BZ-X700 also acquired time-lapse imaging. For the cell culture experiment with conditioned media, newly replaced media (Macrophage SFM+10% FBS) were collected and used after 72-h exposure to CAMs or MDCAFs. For the MDCAF-transdifferentiation inhibition experiment (Fig. 4), the same number of macrophages from cavity fluid was cultured in each indicated condition. All cells were harvested and analyzed by FACS after 3 weeks of culture.

2.4. FACS analysis and cell isolation

Cells were resuspended with FACS buffer (PBS containing 2% FBS and 1 mM EDTA) at a concentration of 1×10^7 cells/mL, incubated with FcR blocking reagent (Miltenyi Biotech) and Tru-Stain Monocyte Blocker (BioLegend) for 15 min at 4 °C to block unspecific stain and subsequently stained with the following antibodies for 30 min at 4 °C: FITC-conjugated anti-CD14, PE/Cy7-conjugated anti-CD34, APC-conjugated anti-CD45, BV421-conjugated anti-CD68, APC-conjugated anti-CD80, APC-conjugated anti-CD86, PE/Cy7-conjugated anti-CD90, PE-conjugated anti-CD163, and FITC-conjugated *anti*-HLADR (BioLegend). Stained cells were washed with FACS buffer, analyzed, and sorted with FACS Aria III.

2.5. Isolation of $CD14^+$ cells

$CD14^+$ macrophages within cavity fluids were isolated by magnetic separation. CD14 beads (Miltenyi Biotech) were used according to the manufacturer's instructions. The purity of isolated $CD14^+$ macrophages was analyzed by FACS and was an average of 94%.

2.6. cDNA microarray analysis

The global transcriptome was analyzed by SurePrint G3 Human GE microarray 8 × 60K Ver. 3.0 (Agilent Technologies). Then, 1×10^4 cells of each population were sorted by FACS and lysed with TRIzol (Thermo Fisher Scientific). Total RNA was extracted according to the manufacturer's instructions. The cRNA of mRNA from each sample was synthesized with the Low Input Quick Amp Labeling Kit (Agilent Technologies), and 600 ng of cRNA were hybridized to microarray chip and scanned with an Agilent SureScan Microarray Scanner. The scanned image was processed with Feature Extraction software (Agilent Technologies). The obtained gene expression data were analyzed with GeneSpring GX software (Agilent Technologies). Differentially expressed genes were selected that passed a paired *t*-test $p < 0.01$ with Storey bootstrapping and $\log_2$ fold change>5.0.

2.7. Quantitative PCR

cDNA synthesis was performed using the reverse transcriptase SuperScript VILO cDNA Synthesis Kit (Thermo Fisher Scientific). Quantitative PCR (qPCR) of target genes was performed using TB Green Premix Ex *Taq*II, ROX plus (TAKARA BIO INC.) on StepOnePlus Realtime PCR System (Applied Biosystems). The thermal cycling procedures were as follows: Incubation at 95 °C for pre-denaturation for 30 s, followed by 50 cycles with denaturation at 95 °C for 15 s, and annealing at 60 °C for 60 s. GAPDH was used as the internal control. The primer sequences used were listed in Supplementary Table 1.

2.8. Whole exome sequencing

$CD34^+$ cells were isolated magnetically from bone marrow aspirates with MACS CD34 beads (Miltenyi Biotech). The purity of isolated cells was confirmed to be 80.7% by FACS. Total DNA was extracted with QIAmp DNA micro (Qiagen) according to the manufacturer's instructions. Extracted DNA was quantified with a Qubit ds DNA HS assay kit (Thermo Fisher Scientific), and 9.06 ng of DNA were pre-amplified with REPLI-g UltraFast Mini (Qiagen). Amplified DNA (1 μg) was sheared ultrasonically by M220 (Covaris) to 300 bp, which is optimal for target enrichment. Adapter-ligated libraries were amplified with PCR using KOD plus neo (TOYOBO). Targeted exons were enriched with SureSelect Human All Exon V6 (Agilent Technologies) according to the manufacturer's instruction. The captured libraries were PCR amplified with indexing primers and then size-selected by SPRIselect (Beckman

Coulter) to 300–500 bp. The libraries were sequenced on Illumina Hiseq 2500 using 100-bp paired-end mode (Illumina).

2.9. Read mapping and somatic mutation detection

Raw sequencing data were aligned to the reference human genome (hg19) using Burrow-Wheeler Aligner Maximal Exact Match (bwa-mem) [14], version 0.7.12, with default parameter settings. Alignments were sorted and converted to BAM format with GATK (version 3.5) and SAMtools (version 1.4.1) [15]. The VarScan2 (version 2.3.7) [16] algorithm was implemented to identify somatic single nucleotide variants (SNVs) and indels for matched samples. Called candidate SNVs and indels with at least 10 somatic variant-supporting reads and variant allele frequencies in tumor samples $\geq$0.1 were further manually curated using integrative genomics viewer [17] and subjected to validation using amplicon-sequencing.

2.10. Immunohistochemistry, immunofluorescence, and immunocytochemistry

Human biopsy samples and implanted tumors from xenografts were fixed in either 10% formalin or 4% paraformaldehyde, embedded in paraffin, and cut into 2-μm-thick sections. The following primary antibodies were used: anti-CD45 (1:200, Cell Signaling TECHNOLOGY), anti-CD90 (1:200, Sigma-Aldrich), *anti*-αSMA (1:100, Abcam), *anti*-GFP (1:500, BML), FITC-conjugated anti-CD14 (1:50, BioLegend), and PE-conjugated anti-CD90 (1:50, BioLegend). Primary antibodies were incubated at room temperature for 30 min in a humidified chamber. For immunohistochemistry, the sections were subsequently incubated with HRP-conjugated secondary antibodies (EnVision, Dako) for 30 min. Diaminobenzidine (ImmPACT DAB, Vector Laboratories) was used as the chromogen, and slides were counterstained with Mayer's hematoxylin. For immunofluorescence, Alexa fluor 488 or 594 secondary antibodies (Invitrogen) were used at room temperature for 30 min, and then slides were counterstained with 4′, 6-diamidino-2-phenylindole (Sigma-Aldrich). The opal manual IHC kit (PerkinElmer) was also used as an alternative method for immunofluorescence. For immunocytochemistry, after fixation with 4% paraformaldehyde for 1 min, cells were stained with fluorescence-conjugated antibodies for 30 min and then counterstained with 4′, 6-diamidino-2-phenylindole. The immunofluorescence images were acquired with confocal microscopy (A1, Nikon) or a Mantra quantitative pathology workstation (PerkinElmer) for immunofluorescence. For immunocytochemistry, images were acquired using an Axio Examiner D1 microscope (Zeiss) with a confocal scanner unit, CSUW1CU (Yokogawa).

2.11. Animal experiment

C57BL/6.Rag2^{null}Il2rg^{null}NOD-Sirpa (BRGS) mice were immunodeficient mice developed in our laboratory, as described previously [18]. All mice were bred and maintained under specific pathogen-free conditions at the Kyushu University Animal Facility. All animal studies and procedures were approved by the ethics committees at Kyushu University. DLD-1 cells with or without the same number of MDCAFs were resuspended in Matrigel (Corning), and were injected both flanks of BRGS mice subcutaneously. The mice were sacrificed with sevoflurane and cervical dislocation, and the engrafted tumor was harvested. DLD1/AkaLuc cells were also inoculated in the same procedure. The mice were anesthetized with 2% isoflurane, and the bioluminescence images were acquired using an IVIS Spectrum (Caliper Life Sciences) 15 min after the administration (ip) of 100 μl of 1 mM AkaLumine-HCl.

2.12. Statistical analysis

Data are presented as the means plus or minus standard deviation. The significance of differences between groups was determined by Student's *t*-test for two groups and the Steel-Dwass test for multiple groups. Statistical analysis was performed with JMP Pro (version 13.0.0, SAS) and GeneSpring GX software (Agilent Technologies).

3. Results

3.1. Macrophages in malignant cavity fluid transdifferentiate into fibroblast-like cells in vitro

Peritoneal cancer dissemination promotes peritoneal fibrosis and produces malignant ascites. Surgical specimens of disseminated tumor in peritoneal cavity contain many fibroblasts, as well as tumor cells, but little is known about the origin of these fibroblasts. Furthermore, many leukocytes including macrophages infiltrate around tumor cells and fibroblasts (Fig. 1A). We hypothesized that these fibroblasts and macrophages have a close relationship and that some fibroblasts are derived from macrophages. To this end, this study focused on malignant ascites and pleural effusions from patients with digestive organ cancers to investigate the differentiation properties of macrophages within cavity fluid (Fig. 1B; patients' characteristics are summarized in Supplementary Table 2). Flow cytometer analyses showed that macrophages within fluid express leukocyte marker CD45 and monocyte/macrophage marker CD14. Fibroblast-like cells were defined as CD45-negative and CD90-positive, which is recognized as a common mesenchymal cell marker [19]. Macrophages are abundant and constitute 10%–30% of the total cells in most cases, whereas very few CD90-positive fibroblast-like cells are observed. Cells from cavity fluid were sorted to three fractions exclusively: the $CD45^{+}CD14^{+}$ macrophage fraction, the $CD45^{-}CD90^{+}$ fibroblast-like cell fraction, and the remaining fraction. Isolated cells were cultured with 10% fetal bovine serum (FBS). Cultured cells were harvested and analyzed again by FACS after 3–4 weeks of incubation. Surprisingly, $CD90^{+}$ fibroblast-like cells that exhibited spindle shapes newly emerged only from the $CD45^{+}CD14^{+}$ macrophage fraction, whereas the initially $CD45^{-}CD90^{+}$ fibroblast-like cells did not expand (Fig. 1C). These fibroblast-like cells that emerged from macrophages were defined as MDCAFs (macrophage-derived CAFs). These macrophages initially expressed other common macrophage markers such as CD68 and CD163. They also possessed phagocytic activity (Supplementary Figs. 1A and B). These macrophages were called CAMs (cavity fluid-associated macrophages). Immunocytochemistry images showed the CAM to MDCAF transdifferentiation process. MDCAFs lose CD14 expression and then start to express CD90, form spindle shapes, and adhere to plate surfaces as well as fibroblasts (Fig. 1D). Time-lapse imaging showed CAMs form spindle shape and divide quite slowly, but cell fusion was not observed (Supplementary Fig. 2). These results collectively suggest that macrophages in cavity fluid have potent properties to transdifferentiate into fibroblast-like cells.

3.2. Profiling of macrophages in cavity fluid and macrophage-derived CAFs

Subsequently, transcriptome analysis by cDNA microarray was conducted to investigate whether these $CD90^{+}$ MDCAFs have fibroblast-specific properties. Four pairs of CAMs and MDCAFs established from 4 different patients' samples were analyzed. There was a huge difference in global gene expression between CAMs and MDCAFs (Fig. 2A). CAMs expressed the M2 macrophage marker *CD163*, and MDCAFs expressed the common fibroblast marker *ACTA2* (αSMA) [20] (Fig. 2B). A fibroblast-specific gene set and a macrophage-specific gene set were constructed from the literature [21–23] (Supplementary Table 3), and gene set enrichment analysis (GSEA) was conducted on these gene sets to validate the properties of each cell. As expected, fibroblast-specific genes were enriched in MDCAFs, whereas macrophage-specific genes were enriched in CAMs. GSEA also showed enrichment of signaling by TGFβ receptor complex in MDCAF (Fig. 2C). Gene ontology analysis via Metascape was conducted on each of the top 500 ranked genes with

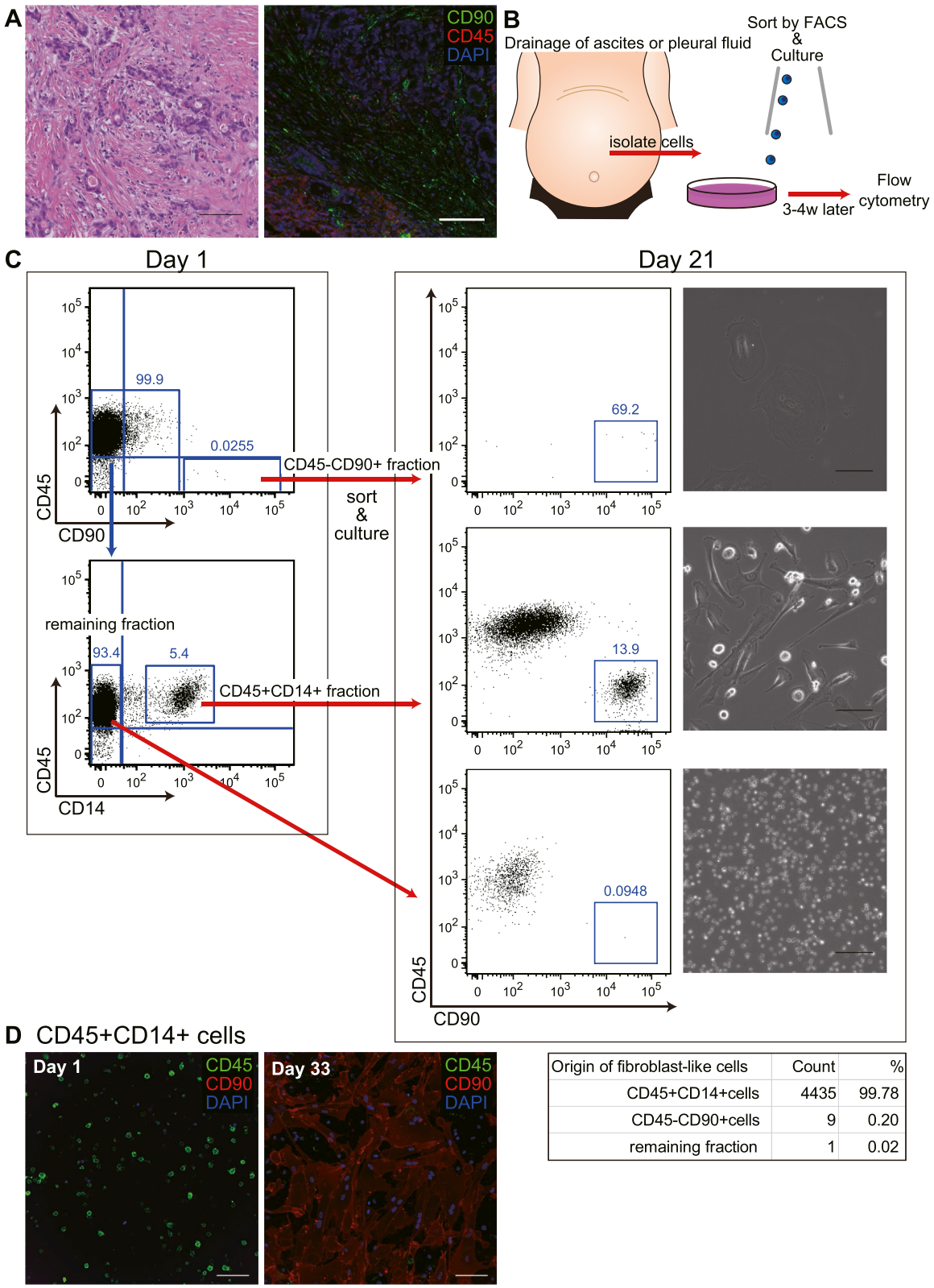

Origin of fibroblast-like cells	Count	%
CD45+CD14+cells	4435	99.78
CD45-CD90+cells	9	0.20
remaining fraction	1	0.02

Fig. 1. Macrophages in ascites/pleural effusions from cancer patients are primed to transdifferentiate into fibroblast-like cells in vitro culture.
(A) Representative image of peritoneally disseminated tumor from colon cancer, accompanied by abundant fibroblasts (CD90-positive cells) and leukocytes (CD45-positive cells). HE stain and immunofluorescence image. **(B)** Schematic image of macrophages within cavity fluid collection and culture. **(C)** Flow cytometry plot of cells in cavity fluid soon after collection and after 3 weeks of culture. Only from the $CD14^{+}$ macrophage fraction, $CD90^{+}$ fibroblast-like cells emerged. The table shows the proportion of the source of $CD45^{-}CD90^{+}$ fibroblast-like cells after culture. **(D)** Immunofluorescence image of isolated and cultured macrophages. Cells from the same sample (A108) are stained at day 3 and day 33. Scale bar, 100 μm.

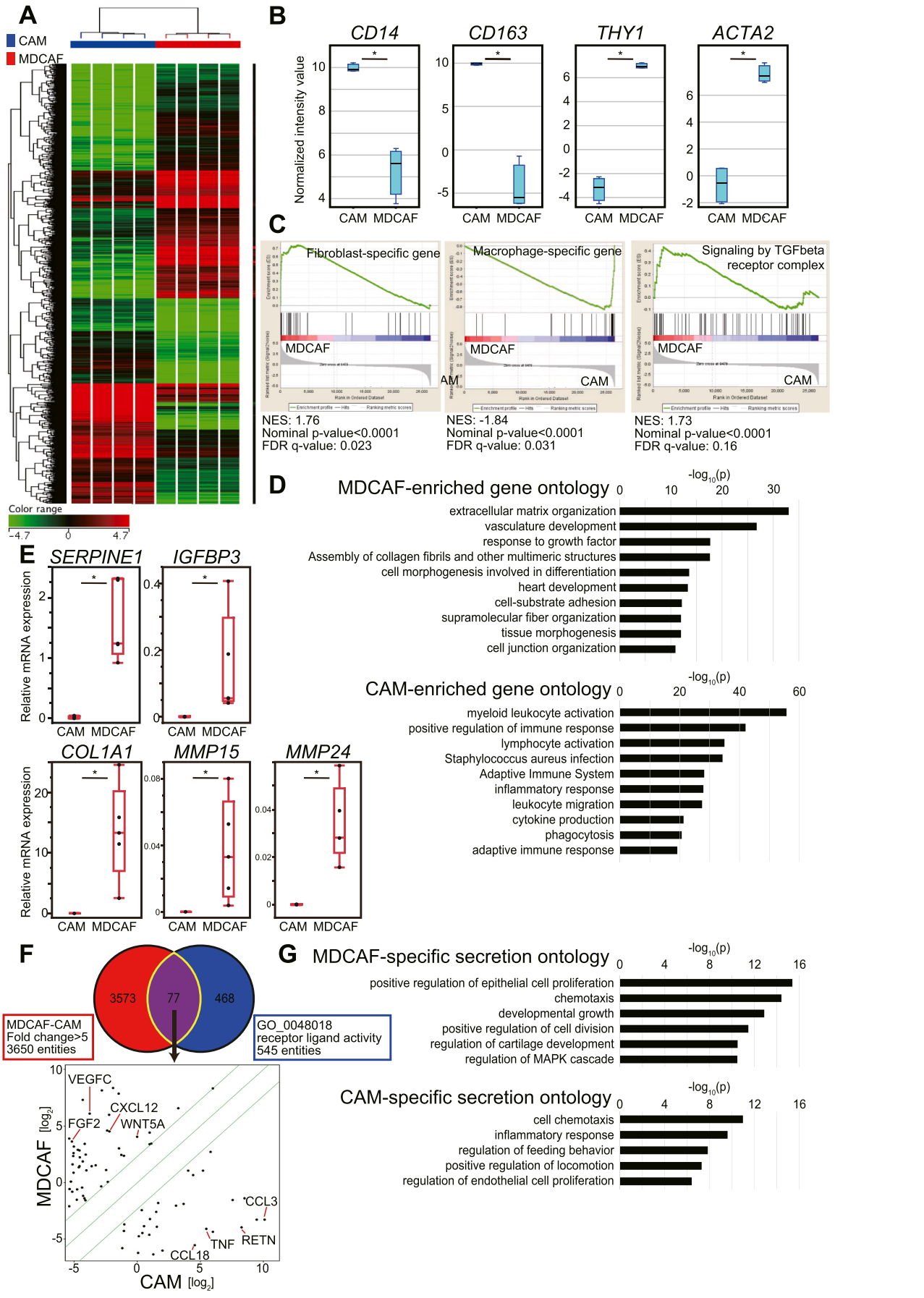

(caption on next page)

Fig. 2. Transcriptome analysis of cavity fluid-associated macrophages (CAMs) and macrophage-derived cancer-associated fibroblasts (MDCAFs) induced by in vitro culture.
(A) Four pairs of CAMs and MDCAFs (A90, A109, A110 and A115) were analyzed. Hierarchical clustering is displayed as a heat map of log_2-transformed signal values. **(B)** gene expressions of representative markers of macrophages (*CD14*, *CD163*) and fibroblasts (*THY1*, *ACTA2*). *$p < 0.05$ with Student's *t*-test **(C)** Gene set enrichment analysis for CAMs and MDCAFs. NES, normalized enrichment score. **(D)** Gene ontology analysis via Metascape for top 500 ranked differentially expressed genes in MDCAFs and CAMs. **(E)** Quantitative PCR confirmed MDCAF expressed TGFβ signaling marker (*SERPINE1, IGFBP3*) and Collagenous fiber/extracellular matrix genes (*COL1A1, MMP15, MMP24*). **(F)** Venn diagram showing significant changes in secreting factor gene expressions due to transdifferentiation. Selected genes are displayed in a scatter plot and Table 1. **(G)** Gene ontology analysis via Metascape for the 77 selected genes in (**F**).

highest fold-change among differentially expressed genes between CAMs and MDCAFs in order to investigate the changes of cell biology [24]. In MDCAFs, gene ontology of extracellular matrix organization, vasculature development, and response to growth factor were enriched. On the other hand, gene ontology of myeloid leukocyte activation and positive regulation of immune response were enriched in CAMs (Fig. 2D). Quantitative PCR with another sample set confirmed that MDCAFs expressed *SERPINE1* and *IGFBP3*, known as TGFβ signaling marker [25–27]. Collagenous fiber and extracellular matrix were also highly expressed in MDCAFs (Fig. 2E).

Generally, TAMs and CAFs residing inside of tumors are known to support tumor growth by secreting cytokines and growth factors. To investigate differences in cell function, secreting factor gene expressions were assessed. Genes differentially expressed with more than 5 times fold-change between two cell types were selected. Among them, genes annotated as having receptor ligand activity by AmiGO2 were further extracted [28–30] (Fig. 2F). Twenty-five secreting factors were enriched in CAMs, and 45 genes were enriched in MDCAFs (Table 1). Gene ontology analysis was conducted on these specifically expressed genes. The term "positive regulation of epithelial cell proliferation, developmental growth" was ranked in MDCAFs, which suggests that MDCAFs have the capability to promote epithelial tumor growth (Fig. 2G).

3.3. MDCAFs promotes tumor progression in vitro and in vivo

Whether MDCAFs promote tumor progression was investigated. A cell culture experiment with conditioned media from CAMs and MDCAFs was performed. A colon cancer cell line (DLD-1), a gastric cancer cell line (NUGC4), and a pancreatic cancer cell line KMOA103 (our newly established cell line from pancreatic cancer) were cultured with these CAM-conditioned media, MDCAF-conditioned media or control media. MDCAF-conditioned media significantly enhanced proliferation activity in all three cell lines while CAM-conditioned media promote cell growth to some extent (Fig. 3A).

Subsequently, a xenograft experiment was conducted to evaluate MDCAFs' tumor promoting ability in vivo. $CD90^+$ MDCAFs were sorted and inoculated into immunodeficient mice with the same cell number of colon cancer cell line DLD-1 (Fig. 3B). DLD-1 cells with MDCAFs formed significantly larger tumors than DLD-1 cells alone (Fig. 3C and D). These DLD-1 cells were engineered to continuously express GFP in advance, and immunofluorescent microscopy images showed that these engrafted tumors consisted mostly of tumor cells, not MDCAFs (Fig. 3E).

Interestingly, MDCAFs promoted tumor growth although microscopic images of engrafted tumors showed most MDCAFs could not persist in the xenograft model. We presumed MDCAFs give tumor protective niche and support tumor growth initially. We conducted in vivo bioluminescence imaging to observe the early growth advantage of co-transplanted tumors. AkaBLI is one of the bioluminescence imaging systems composed of AkaLumine-HCl (substrate) and AkaLuc (Luciferase), which is quite bright enough to detect minimal cell numbers [31]. We engineered AkaLuc-expressing DLD-1 cells and conducted the xenograft experiment in the same manner (Fig. 3F). As expected, co-transplanted tumors achieved earlier engraftment than DLD-1 cells alone (Fig. 3G and H). When MDCAFs were inoculated alone, MDCAFs did not form tumors.

Table 1
Cell type-specific secretion in CAMs and MDCAFs.

CAM-specific secretion factor genes					
AGRP	*CCL18*	*CCL23*	*CCL3*	*CCL8*	*CMTM1*
CXCL16	*GDF7*	*GHRL*	*GMFG*	*HGF*	*IL10*
IL16	*IL1RN*	*IL27*	*LTB*	*NRP1*	*RETN*
SPP1	*TNF*	*TNFSF12*	*TNFSF13*	*TNFSF8*	*TRH*
VSTM1					
MDCAF-specific secretion factor genes					
APLN	*BDNF*	*BMP1*	*BMP2*	*BMP4*	*CD320*
CTF1	*CXCL12*	*EDN2*	*EFEMP1*	*EPGN*	*FGF1*
FGF2	*FGF7*	*FGF9*	*FLRT2*	*FLRT3*	*GDF15*
GDF5	*IL32*	*IL33*	*INHBB*	*LDOC1*	*LIF*
MAPT	*MDK*	*NPPB*	*NPY*	*PTHLH*	*PTN*
SAA1	*SAA2*	*SCG2*	*SCGB3A1*	*SEMA3A*	*SEMA3F*
STC2	*TGFB2*	*TNFRSF11B*	*UTS2B*	*VEGFC*	*WNT4*
WNT5A					

3.4. TGFβ and cell-matrix adhesion is required for MDCAF growth from CAMs

In previous experiments, CAM to MDCAF transdifferentiation was induced under 10% FBS-supplemented media. This change was markedly attenuated when cultured in the FBS-reduced condition (Fig. 4A and B). Reactome analysis from a previous microarray dataset showed enrichment of signaling by TGFβ receptor complex (Fig. 2C). It was assumed that TGFβ signaling is involved in this transdifferentiation, because we previously reported that TGFβ is abundant in malignant ascites [32].

An identical number of CAMs was cultured in 2% FBS-supplemented media, with TGFβ and with TGFβ plus TGFβ inhibitor (SB431542). After three weeks of culture, TGFβ expanded MDCAF growth from macrophages, and the TGFβ inhibitor abrogated this expansion (Fig. 4A, C).

Interestingly, floating $CD90^+$ fibroblast-like cells were rarely observed in cavity fluid, although CAMs are able to transdifferentiate to MDCAFs (Fig. 1C). A microarray dataset also shows enrichment of cell-substrate adhesion (Fig. 2C). We hypothesized that CAMs cannot transdifferentiate into MDCAFs as long as they are floating in cavity fluid. Cell adhesion might promote this transdifferentiation. From this point of view, cell transdifferentiation ability was then compared on a normal collagen-coated plate or an ultra-low attachment plate. On the ultra-low attachment plate, cells cannot adhere to the plate surface. As expected, macrophages could not transdifferentiate to fibroblast-like cells on the ultra-low attachment plate (Fig. 4D and E). Some study shows glucocorticoids are potent inhibitors of fibroblast growth and activity [33]. The addition of dexamethasone attenuated MDCAF transdifferentiation from macrophages. (Supplementary Fig. 3). TGFβ signaling and cell adhesion are required for CAM to MDCAF transdifferentiation.

3.5. Clonal hematopoiesis shows that MDCAFs originate from bone marrow

We hypothesized that these MDCAFs might originate from hematopoietic stem cells (HSCs). Recent studies have shown that hematopoietic stem cells with somatic mutations expand clonally during human aging, and this clonal expansion is associated with increased risks of subsequent hematologic malignancies and various diseases [34,35]. This potentially abnormal hematopoiesis is termed clonal hematopoiesis of

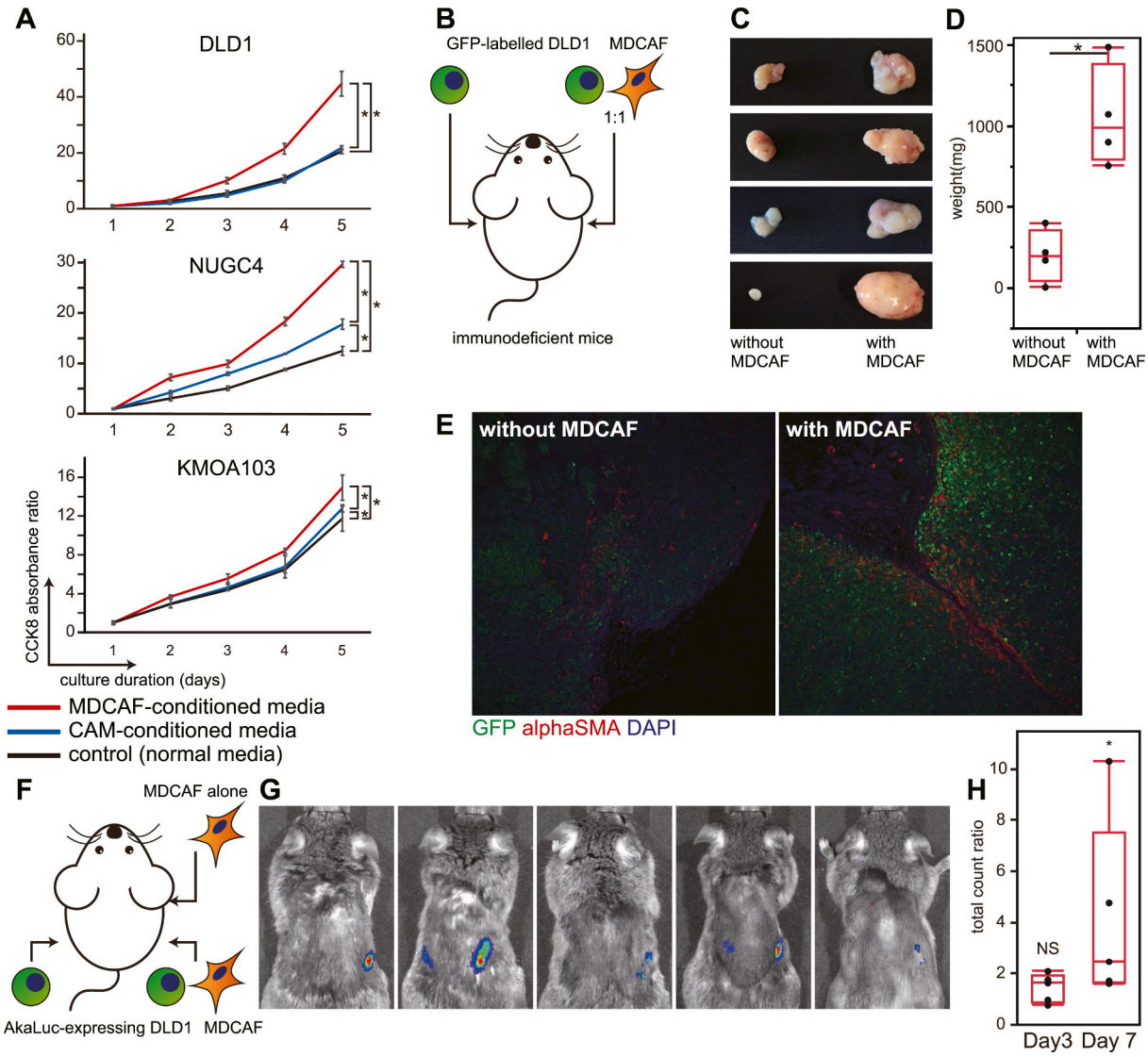

Fig. 3. MDCAFs promote tumor progression in vitro and vivo.
(A) CCK8 assay for assessing tumor cell line growth. DLD-1 (colon cancer), NUGC4 (gastric cancer), and KMOA103 (pancreatic cancer) were cultured in CAM-conditioned media, MDCAF-conditioned media (A224) or normal media. the absorbance ratio to day1 were plotted. *p < 0.05 with Student's *t*-test. **(B)** Schematic image of xenograft experiment. Xenotransplanted mice were sacrificed at day 33. **(C)** Macroimage of implanted DLD-1 cells. **(D)** Weight of implanted DLD-1 cells, *p < 0.05 with Student's *t*-test. **(E)** Representative image of xenotransplanted tumor by immunofluorescence staining. Fibroblast-like cell expansion was not observed. **(F)** Schematic image of xenograft experiment for bioluminescent imaging. **(G)** Representative bioluminescence images 7days after inoculation. **(H)** The relative value of total photon count from DLD-1 cells and MDCAFs inoculated region compared to DLD-1 cells inoculated region. *p < 0.05 with Wilcoxon rank sum test.

indeterminate potential (CHIP). We used CHIP to track the origin of MDCAFs.

To validate this theory, a pleural effusion sample from a patient with cancer and hematologic malignancy was used. Case P30 had esophageal squamous cell carcinoma and myelodysplastic syndrome (refractory cytopenia with multi-lineage dysplasia). MDCAFs and macrophages in pleural fluid are supposed to share the same genetic alterations with HSCs if they are derived from circulating monocytes. $CD34^{+}$ hematopoietic stem/progenitor cells (HSPCs) of case P30 were isolated from bone marrow. MDCAFs were induced from the CAMs in the pleural effusion in the same manner. Nail clippings were used as a germline control (Fig. 5A). Whole exome sequencing detected the *MAP1A* variant in HSPCs. Sanger sequencing confirmed that macrophages and MDCAFs harbored the same *MAP1A* variant, as expected. In contrast, nail clippings did not share this variant (Fig. 5B). Target amplicon sequencing showed that macrophages and MDCAFs possess this variant allele with a similar frequency (Fig. 5C). This result indicated that macrophages in pleural effusion originate from HSPCs and then transdifferentiate to MDCAFs. These findings also proved that the emergence of these MDCAFs is not due to contamination of residual fibroblasts in cavity fluid, because germline cells, nail clippings, did not share this variant with HSPCs, macrophages, and MDCAFs.

Biopsy specimens from primary sites of esophageal cancer were also analyzed. Fibroblasts in the primary site were immunohistochemically stained with *anti*-αSMA antibody and micro-dissected. The same *MAP1A* variant were also seen in these fibroblasts (Fig. 5D). This result showed that some fibroblasts in the primary cancer site were also derived from HSPCs.

In conclusion, CAMs in malignant effusions are derived from hematopoietic stem cells and acquire a fibroblast-like phenotype as MDCAFs. This transdifferentiation is promoted in the surrounding microenvironment that produces TGFβ and extracellular matrix.

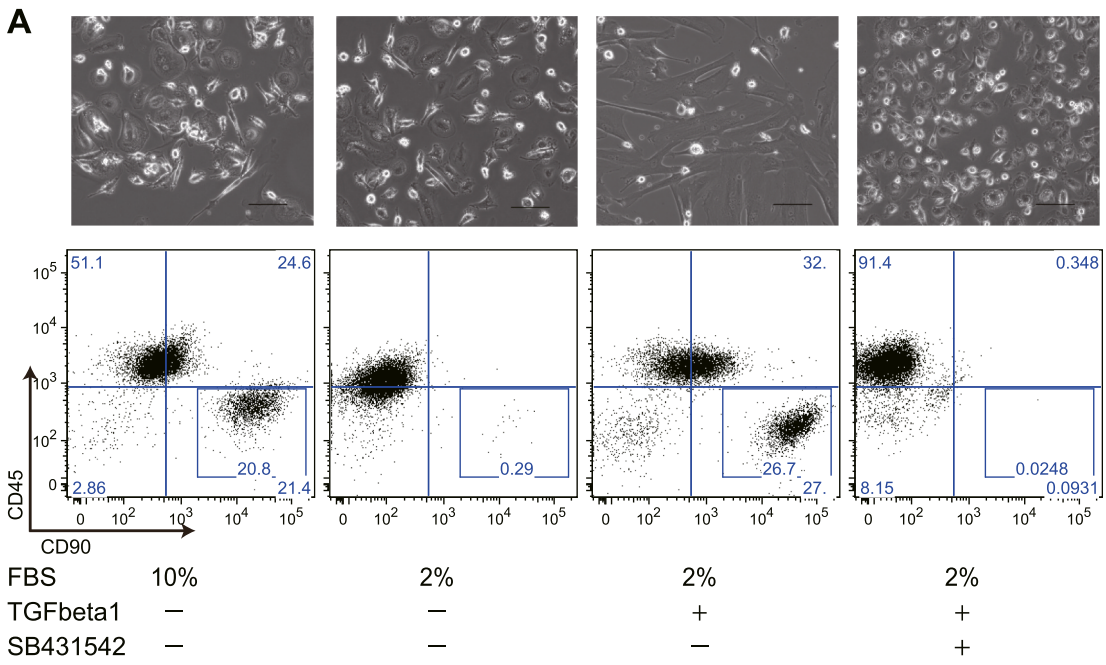

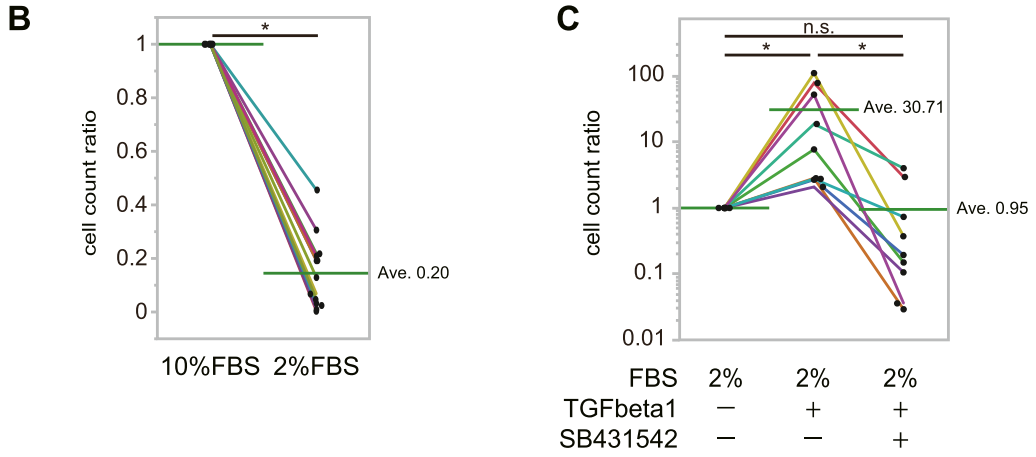

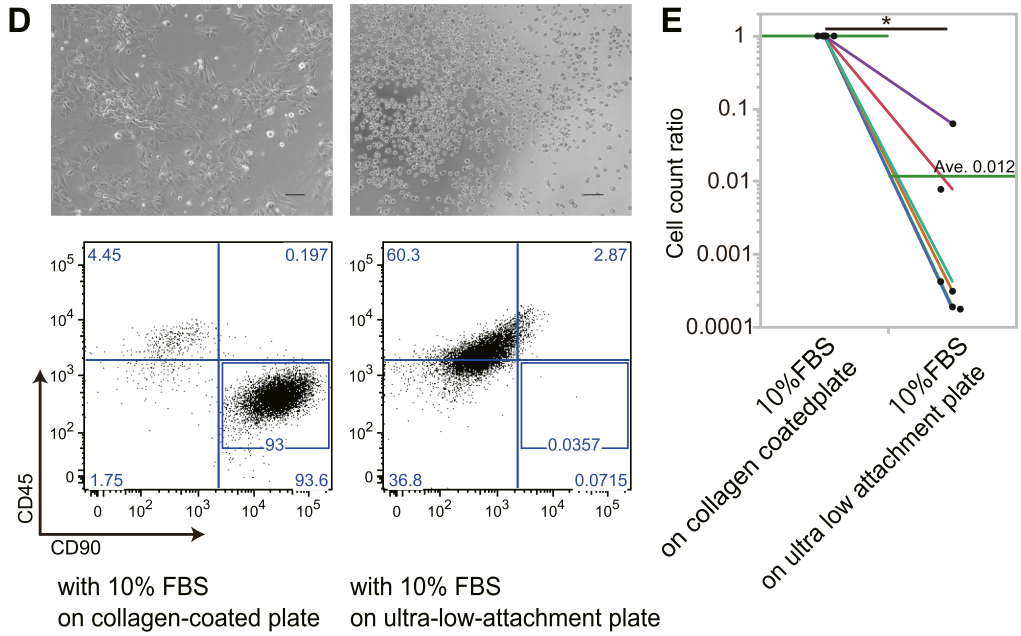

(caption on next page)

Fig. 4. Serum, TGFβ and cell-adhesion induces MDCAF growth from CAMs.
(A) Representative bright field images and flow cytometry plots of cultured CAMs in each conditions. **(B–C)** The cell count ratio is displayed. The total cell counts of CD45–CD90+MDCAFs cultured with 2% FBS were set as standard. *p < 0.05 with Student's *t*-test in (B), and Steel-Dwass test in (C). **(D)** Cell-adhesion is required in MDCAF growth from CAMs. Representative bright field images and flow cytometry plots of cultured CAMs. **(E)** The cell count ratio is displayed in the same manner as (B–C). *p < 0.05 with Student's *t*-test.

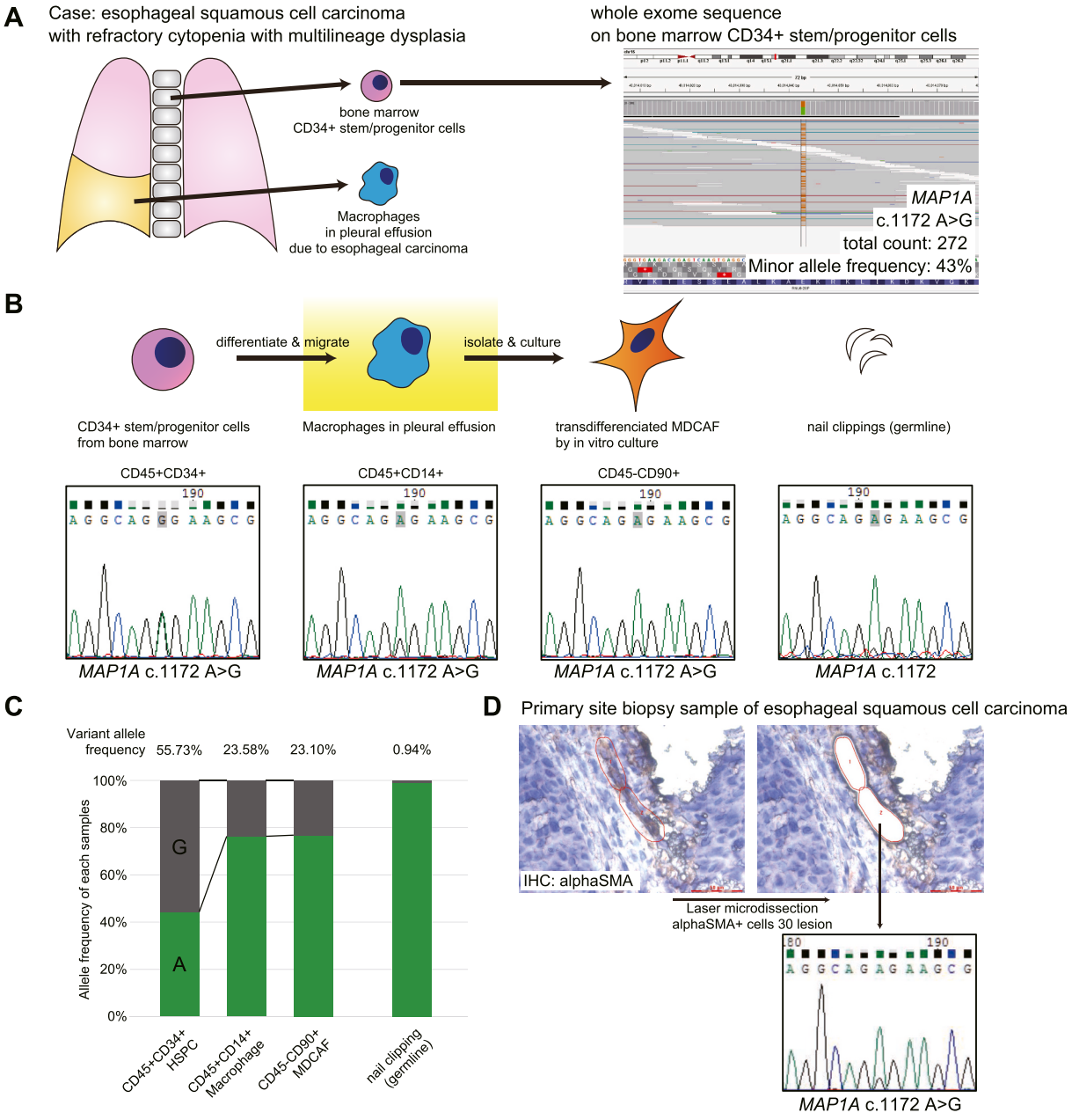

Fig. 5. Clonal hematopoiesis shows that MDCAFs originate from bone marrow.
(A) Whole exome sequencing of $CD34^{+}$ hematopoietic stem/progenitor cells (HSPC) from bone marrow aspiration of case P30. *MAP1A* somatic single nucleotide variant is detected in HSPC. **(B)** Sanger sequencing of *MAP1A* c.1172 A > G variant in each sample, CD34+HSPC from bone marrow, macrophages in cancer-associated pleural fluid and transdifferentiated MDCAFs via in vitro culture. Nail clippings referred to as germline. **(C)** Variant allele frequency of each PCR amplicon analyzed by deep sequencing. **(D)** Sanger sequencing of fibroblasts in a primary esophageal cancer biopsy FFPE sample. Fibroblasts are detected with *anti*-αSMA IHC staining. Thirty regions of αSMA-positive cells were collected by laser microdissection.

MDCAFs secrete various growth factors and promote tumor progression (Fig. 6).

4. Discussion

Generally, fibroblasts are recognized as elongated cells that show a fusiform or spindle-like shape, adhere to plastic, and produce much collagenous fiber. However, the definition of fibroblasts is still poorly established in molecular terms. Although several markers of fibroblasts are proposed, none of them are exclusive to fibroblasts [20]. Fibroblasts are potentially heterogeneous, and they might be an aggregation of a variety of cell types [36]. Recently, heterogeneity of cancer-associated

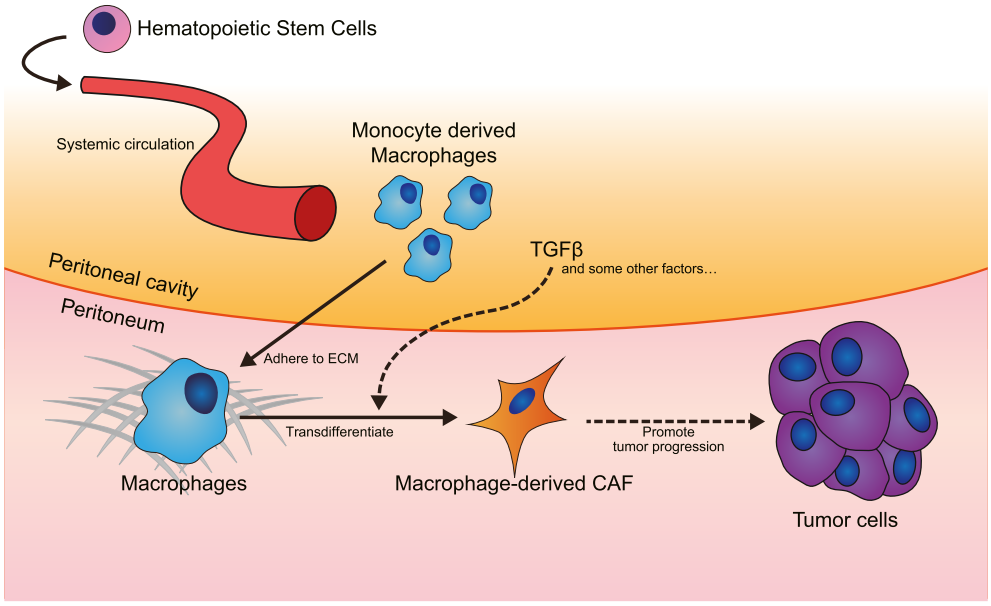

Fig. 6. Graphical summary of CAM to MDCAF transdifferentiation in the tumor microenvironment.

fibroblasts has been gradually recognized due to development of single-cell analysis [21]. Lee et al. reported that mesenchymal cell heterogeneity was important in lung development. Different mesenchymal cell types maintain their neighboring distinct epithelial cells, airway cells, and alveolar cells [37]. These findings indicate the importance of mesenchymal cell diversity as niche cells to develop complex organs. However, how CAF heterogeneity affects the tumor microenvironment is not well known. Understanding the origins of fibroblasts might be one of the important keys to understanding CAF heterogeneity.

There is a close relationship between macrophage accumulation and fibrosis. Many studies have reported that macrophages induce fibrosis through recruitment and activation of residential fibroblasts [38]. However, a new concept is emerging that macrophages acquire a fibroblast-like phenotype and induce fibrosis directly, mainly in fibrotic disease research fields such as renal fibrosis or myocardial infarction [11–13]. David et al. showed a macrophage-myofibroblast transition in a fibrotic kidney disease model. In an experimental renal fibrosis model with GFP + bone marrow-transplanted mice, GFP + F4/80+ macrophages migrated into injured kidney and transdifferentiated to αSMA + myofibroblasts [11]. Similarly in an experimental myocardial infarction model, GFP + bone marrow-transplanted mice showed accumulation of GFP + myofibroblasts at the injured heart muscle area [39]. Previously, CAFs were thought to be derived from stromal cell progenitors [4]. Several studies showed that some components of CAFs were recruited from bone marrow. They concluded that these CAFs originate from circulating mesenchymal stem cells [40,41], but the present study showed that macrophages in malignant ascites and pleural effusions transdifferentiate to fibroblast-like cells that acquire a similar phenotype to cancer-associated fibroblasts. This transdifferentiation depended on TGFβ signaling and cell-matrix adhesion. This transdifferentiation process may contribute to tumor progression and fibrosis in the involved organ. Genomic tracing in a patient with MDS showed that hematopoietic stem cells and circulating monocytes differentiate to macrophages in cavity fluid and then transdifferentiate to fibroblast-like cells. TAMs and CAFs are considered important cells in the tumor microenvironment, and functional analysis of each cell had been reported independently. The present report brings the new insight that some components of these cells share the same progenitor.

Many reports have shown that patients with CAF-rich cancer have poor survival [42]. There is a vicious cycle between tumor cells and CAFs, that is, tumor cells contribute to CAF development, and CAFs promote tumor cell proliferation. Recent transcriptome analyses classified colorectal cancer into several subtypes according to gene expression [43–46]. Claudio et al. reclassified several transcriptome datasets of colorectal cancer into TA/enterocyte subtype, goblet/inflammatory subtype, and stem/serrated/mesenchymal (SSM) subtype. They showed that SSM subtype is associated with high stromal content and a poor prognosis, and that the SSM gene signature depends on stromal cells [47]. In their report, gene signatures of purified tumor cells from the SSM subtype cancer were the same as those of tumor cells from the TA/enterocyte or goblet/inflammatory subtype cancer. The difference in gene signatures between the SSM subtype and other subtypes was based on stromal cells of the tumor microenvironment. In addition, they showed that the stromal amount in cancer was one of the independent prognostic factors. These results suggest that CAF recruitment depends on the host reaction to tumor cells, but not the tumor cell itself. In the present study, there were some differences in transdifferentiation ability from CAMs to MDCAFs among the samples. This variation might reflect differences in fibrogenic potential in cancer as a host reaction in each individual.

Generally, TAMs are also recognized as a heterogeneous cell population. Residential tissue macrophages and monocyte-derived macrophages mingle in the tumor microenvironment [48]. Macrophages themselves have dynamic plasticity and a broad spectrum in their function. Their diversity is not limited in the M1/M2-macrophage paradigm, and they can transit to different phenotypes easily [2]. Most macrophages in cavity fluid express CD163 and possess an M2-like phenotype, but which subpopulation among these M2-like macrophages skews to MDCAFs is still not known. Further phenotyping is needed to detect MDCAF progenitors. Transcriptome analysis showed that macrophages enhance the inflammatory response, whereas MDCAFs directly promote tumor cell proliferation. This indicates that CAMs and MDCAFs play different roles in the tumor microenvironment before and after transdifferentiation. In addition, we showed that HSCs and monocytes are able to transdifferentiate to MDCAFs. Therefore, monocytes can be one of the potent progenitors of fibrotic cells. Clarifying this transdifferentiation mechanism might help regulate the fibrogenic process not only in cancer, but also in other fibrotic diseases. The present results showed that MDCAFs carry genetic alterations due to CHIP. Recently, some reports have shown that CHIP is associated with risk for several

diseases, not only hematological malignancies. Jaiswal et al. reported that CHIP is one of the independent risk factors for cardiovascular disease [35]. An in vivo experiment using Tet2-knockout transgenic mice showed that Tet2-mutated macrophages express IL-1beta, invade atherosclerotic plaques, and finally promote atherosclerosis [49]. CHIP can affect macrophage function and create conditions predisposing to certain diseases. MDCAFs originating from clonal hematopoiesis might have additional functions favoring cancer.

We have to recognize present study has several limitations. First, macrophages are known to have cell fusion ability in some situations [50]. As our observation, cell fusion of macrophages was not observed in the transdifferentiation process from CAMs to MDCAFs. The possibility of cell fusion cannot be denied entirely, but we consider cell fusion is a rare phenomenon even if there were cell fusion. Second, the long-term effects of MDCAF are not yet clear. We carried out the xenograft experiment to access the tumor-promoting ability of MDCAFs. However, transplanted human stromal cells gradually disappear as the tumor grows, as shown in Fig. 3 and previous reports [51,52]. Bioluminescence imaging demonstrated MDCAFs support tumor growth in the early period, but how MDCAFs work in the late period was not evaluable. Some other experiments may be necessary to resolve these limitations, such as reproducing the CAM-MDCAF transdifferentiation process in transgenic mouse models.

A therapeutic strategy targeting fibroblasts and fibrosis is being developed in several fibrotic diseases [53]. This strategy is promising for cancer therapy to resolve fibrosis and eliminate CAFs. SB431542, a TGFβ inhibitor, inhibited transdifferentiation from macrophages to fibroblast-like cells in the present study. Although SB431542 is not stable in vivo and thus not used as a therapeutic agent in the clinical setting, several drugs that target TGFβ signaling in cancer are being developed [54]. TGFβ signaling is involved in tumor cells themselves, but they are also important factors for regulation of the tumor microenvironment, as shown here [55]. Although some hopeful results of *anti*-TGFβ signaling treatment have been reported, clinical evidence is still not yet established [56,57]. Further evaluation of this strategy is required.

Funding

This research did not receive any specific grant from funding agencies in the public, commercial, or not-for-profit sectors.

Declaration of interests

The authors declare that they have no known competing financial interests or personal relationships that could have appeared to influence the work reported in this paper.

CRediT authorship contribution statement

Mamoru Ito: Conceptualization, Methodology, Investigation, Data curation, Writing – original draft, Writing – review & editing. **Michitaka Nakano:** Investigation, Data curation, Writing – review & editing. **Hiroshi Ariyama:** Writing – review & editing, Supervision. **Kyoko Yamaguchi:** Investigation, Data curation. **Risa Tanaka:** Resources. **Yuichiro Semba:** Software, Formal analysis, Investigation. **Takeshi Sugio:** Formal analysis, Investigation. **Kohta Miyawaki:** Formal analysis, Investigation. **Yoshikane Kikushige:** Writing – review & editing, Supervision. **Shinichi Mizuno:** Supervision, Funding acquisition. **Taichi Isobe:** Supervision, Methodology, Writing – review & editing. **Kenro Tanoue:** Investigation. **Ryosuke Taguchi:** Investigation. **Shohei Ueno:** Investigation. **Takahito Kawano:** Resources, Methodology. **Masaharu Murata:** Resources, Methodology. **Eishi Baba:** Supervision, Project administration, Funding acquisition. **Koichi Akashi:** Supervision, Funding acquisition.

Declaration of competing interest

The authors declare no potential conflicts of interest.

Acknowledgements

This study was supported in part by KMOG, a non-profit organization. The bone marrow samples were provided by G. Yoshimoto from the Department of Hematology, Oncology & Cardiovascular Medicine, Kyushu University.

Appendix A. Supplementary data

Supplementary data to this article can be found online at https://doi.org/10.1016/j.canlet.2022.215597.

References

[1] D. Hanahan, R.A. Weinberg, Hallmarks of cancer: the next generation, Cell 144 (2011) 646–674, https://doi.org/10.1016/j.cell.2011.02.013.
[2] S.K. Biswas, A. Mantovani, Macrophage plasticity and interaction with lymphocyte subsets: cancer as a paradigm, Nat. Immunol. 11 (2010) 889–896, https://doi.org/10.1038/ni.1937.
[3] M. Takeya, Y. Komohara, Role of tumor-associated macrophages in human malignancies: friend or foe? Pathol. Int. (2016) 491–505, https://doi.org/10.1111/pin.12440.
[4] D. Ohlund, E. Elyada, D. Tuveson, Fibroblast heterogeneity in the cancer wound, J. Exp. Med. 211 (2014) 1503–1523, https://doi.org/10.1084/jem.20140692.
[5] R. Kalluri, The biology and function of fibroblasts in cancer, Nat. Rev. Cancer 16 (2016) 582–598, https://doi.org/10.1038/nrc.2016.73.
[6] B. Thibault, M. Castells, J.P. Delord, B. Couderc, Ovarian cancer microenvironment: implications for cancer dissemination and chemoresistance acquisition, Cancer Metastasis Rev. 33 (2014) 17–39, https://doi.org/10.1007/s10555-013-9456-2.
[7] J. Cai, H. Tang, L. Xu, X. Wang, C. Yang, S. Ruan, J. Guo, S. Hu, Z. Wang, Fibroblasts in omentum activated by tumor cells promote ovarian cancer growth, adhesion and invasiveness, Carcinogenesis 33 (2012) 20–29, https://doi.org/10.1093/carcin/bgr230.
[8] C.I. Ripamonti, A.M. Easson, H. Gerdes, Management of malignant bowel obstruction, Eur. J. Cancer 44 (2008) 1105–1115, https://doi.org/10.1016/j.ejca.2008.02.028.
[9] P. Chiarugi, Cancer-associated fibroblasts and macrophages friendly conspirators for malignancy, OncoImmunology 2 (2013) 1–3, https://doi.org/10.4161/onci.25563.
[10] Y. Nie, J. Chen, D. Huang, Y. Yao, J. Chen, L. Ding, J. Zeng, S. Su, X. Chao, F. Su, H. Yao, H. Hu, E. Song, Tumor-associated macrophages promote malignant progression of breast phyllodes tumors by inducing myofibroblast differentiation, Cancer Res. 77 (2017) 3605–3618, https://doi.org/10.1158/0008-5472.CAN-16-2709.
[11] D.J. Nikolic-Paterson, S. Wang, H.Y. Lan, Macrophages promote renal fibrosis through direct and indirect mechanisms, Kidney Int. Suppl. 4 (2014) 34–38, https://doi.org/10.1038/kisup.2014.7.
[12] R.G. Gourdie, S. Dimmeler, P. Kohl, Novel therapeutic strategies targeting fibroblasts and fibrosis in heart disease, Nat. Rev. Drug Discov. 15 (2016) 620–638, https://doi.org/10.1038/nrd.2016.89.
[13] M. Ogawa, A.C. LaRue, C.J. Drake, Hematopoietic origin of fibroblasts/myofibroblasts: its pathophysiologic implications, Blood 108 (2006) 2893–2896, https://doi.org/10.1182/blood-2006-04-016600.
[14] H. Li, R. Durbin, Fast and accurate short read alignment with Burrows-Wheeler transform, Bioinformatics 25 (2009) 1754–1760, https://doi.org/10.1093/bioinformatics/btp324.
[15] M.A. Depristo, E. Banks, R. Poplin, K.V. Garimella, J.R. Maguire, C. Hartl, A. A. Philippakis, G. Del Angel, M.A. Rivas, M. Hanna, A. McKenna, T.J. Fennell, A. M. Kernytsky, A.Y. Sivachenko, K. Cibulskis, S.B. Gabriel, D. Altshuler, M.J. Daly, A framework for variation discovery and genotyping using next-generation DNA sequencing data, Nat. Genet. 43 (2011) 491–501, https://doi.org/10.1038/ng.806.
[16] D.C. Koboldt, Q. Zhang, D.E. Larson, D. Shen, M.D. Mclellan, L. Lin, C. a Miller, E. R. Mardis, L. Ding, R.K. Wilson, VarScan 2 : somatic mutation and copy number alteration discovery in cancer by exome sequencing VarScan 2 : somatic mutation and copy number alteration discovery in cancer by exome sequencing, Genome Res. 22 (2012) 568–576, https://doi.org/10.1101/gr.129684.111.
[17] J.T. Robinson, H. Thorvaldsdóttir, W. Winckler, M. Guttman, E.S. Lander, G. Getz, J.P. Mesirov, Integrative genomics viewer, Nat. Biotechnol. 29 (2011) 24–26, https://doi.org/10.1038/nbt.1754.
[18] T. Yamauchi, K. Takenaka, S. Urata, T. Shima, Y. Kikushige, T. Tokuyama, C. Iwamoto, M. Nishihara, H. Iwasaki, T. Miyamoto, N. Honma, M. Nakao, T. Matozaki, K. Akashi, Polymorphic Sirpa is the genetic determinant for NOD-based mouse lines to achieve efficient human cell engraftment, Blood 121 (2013) 1316–1325, https://doi.org/10.1182/blood-2012-06-440354.
[19] D. Pilling, T. Fan, D. Huang, B. Kaul, R.H. Gomer, Identification of markers that distinguish monocyte-derived fibrocytes from monocytes, macrophages, and

fibroblasts, PLoS One 4 (2009), e7475, https://doi.org/10.1371/journal.pone.0007475.
[20] R. Kalluri, M. Zeisberg, Fibroblasts in cancer, Nat. Rev. Cancer 6 (2006) 392–401, https://doi.org/10.1038/nrc1877.
[21] H. Li, E.T. Courtois, D. Sengupta, Y. Tan, K.H. Chen, J.J.L. Goh, S.L. Kong, C. Chua, L.K. Hon, W.S. Tan, M. Wong, P.J. Choi, L.J.K. Wee, A.M. Hillmer, I.B. Tan, P. Robson, S. Prabhakar, Reference component analysis of single-cell transcriptomes elucidates cellular heterogeneity in human colorectal tumors, Nat. Genet. 49 (2017) 708–718, https://doi.org/10.1038/ng.3818.
[22] M. Beyer, M.R. Mallmann, J. Xue, A. Staratschek-jox, D. Vorholt, W. Krebs, D. Sommer, J. Sander, C. Mertens, A. Nino-castro, S. V Schmidt, J.L. Schultze, High-Resolution Transcriptome of Human Macrophages, 7, 2012, https://doi.org/10.1371/journal.pone.0045466.
[23] M. Heusinkveld, S.H. van der Burg, Identification and manipulation of tumor associated macrophages in human cancers, J. Transl. Med. 9 (2011) 216, https://doi.org/10.1186/1479-5876-9-216.
[24] S. Tripathi, M.O. Pohl, Y. Zhou, A. Rodriguez-Frandsen, G. Wang, D.A. Stein, H. M. Moulton, P. Dejesus, J. Che, L.C.F. Mulder, E. Yángüez, D. Andenmatten, L. Pache, B. Manicassamy, R.A. Albrecht, M.G. Gonzalez, Q. Nguyen, A. Brass, S. Elledge, M. White, S. Shapira, N. Hacohen, A. Karlas, T.F. Meyer, M. Shales, A. Gatorano, J.R. Johnson, G. Jang, T. Johnson, E. Verschueren, D. Sanders, N. Krogan, M. Shaw, R. König, S. Stertz, A. García-Sastre, S.K. Chanda, Meta- and orthogonal integration of influenza "oMICs" data defines a role for UBR4 in virus budding, Cell Host Microbe 18 (2015) 723–735, https://doi.org/10.1016/j.chom.2015.11.002.
[25] R. Rawson, T. Yang, R.O. Newbury, M. Aquino, A. Doshi, B. Bell, D.H. Broide, R. Dohil, R. Kurten, S.S. Aceves, TGF-β1–induced PAI-1 contributes to a profibrotic network in patients with eosinophilic esophagitis, J. Allergy Clin. Immunol. 138 (2016) 791–800, https://doi.org/10.1016/j.jaci.2016.02.028, e4.
[26] L.J. Schedlich, V.M. Yenson, R.C. Baxter, TGF-β-induced expression of IGFBP-3 regulates IGF1R signaling in human osteosarcoma cells, Mol. Cell. Endocrinol. 377 (2013) 56–64, https://doi.org/10.1016/j.mce.2013.06.033.
[27] S. Akiyoshi, M. Ishii, N. Nemoto, M. Kawabata, H. Aburatani, K. Miyazono, Targets of transcriptional regulation by transforming growth factor-β: expression profile analysis using oligonucleotide arrays, Japanese, J. Cancer Res. 92 (2001) 257–268, https://doi.org/10.1111/j.1349-7006.2001.tb01090.x.
[28] S. Carbon, A. Ireland, C.J. Mungall, S. Shu, B. Marshall, S. Lewis, J. Lomax, C. Mungall, B. Hitz, R. Balakrishnan, M. Dolan, V. Wood, E. Hong, P. Gaudet, AmiGO: online access to ontology and annotation data, Bioinformatics 25 (2009) 288–289, https://doi.org/10.1093/bioinformatics/btn615.
[29] S. Carbon, H. Dietze, S.E. Lewis, C.J. Mungall, M.C. Munoz-Torres, S. Basu, R. L. Chisholm, R.J. Dodson, P. Fey, P.D. Thomas, H. Mi, A. Muruganujan, X. Huang, S. Poudel, J.C. Hu, S.A. Aleksander, B.K. McIntosh, D.P. Renfro, D.A. Siegele, G. Antonazzo, H. Attrill, N.H. Brown, S.J. Marygold, P. Mc-Quilton, L. Ponting, G. H. Millburn, A.J. Rey, R. Stefancsik, S. Tweedie, K. Falls, A.J. Schroeder, M. Courtot, D. Osumi-Sutherland, H. Parkinson, P. Roncaglia, R.C. Lovering, R. E. Foulger, R.P. Huntley, P. Denny, N.H. Campbell, B. Kramarz, S. Patel, J. L. Buxton, Z. Umrao, A.T. Deng, H. Alrohaif, K. Mitchell, F. Ratnaraj, W. Omer, M. Rodríguez-López, M.C. Chibucos, M. Giglio, S. Nadendla, M.J. Duesbury, M. Koch, B.H.M. Meldal, A. Melidoni, P. Porras, S. Orchard, A. Shrivastava, H. Y. Chang, R.D. Finn, M. Fraser, A.L. Mitchell, G. Nuka, S. Potter, N.D. Rawlings, L. Richardson, A. Sangrador-Vegas, S.Y. Young, J.A. Blake, K.R. Christie, M. E. Dolan, H.J. Drabkin, D.P. Hill, L. Ni, D. Sitnikov, M.A. Harris, J. Hayles, S. G. Oliver, K. Rutherford, V. Wood, J. Bahler, A. Lock, J. De Pons, M. Dwinell, M. Shimoyama, S. Laulederkind, G.T. Hayman, M. Tutaj, S.J. Wang, P. D'Eustachio, L. Matthews, J.P. Balhoff, R. Balakrishnan, G. Binkley, J.M. Cherry, M.C. Costanzo, S.R. Engel, S.R. Miyasato, R.S. Nash, M. Simison, M.S. Skrzypek, S. Weng, E.D. Wong, M. Feuermann, P. Gaudet, T.Z. Berardini, D. Li, B. Muller, L. Reiser, E. Huala, J. Argasinska, C. Arighi, A. Auchincloss, K. Axelsen, G. Argoud-Puy, A. Bateman, B. Bely, M.C. Blatter, C. Bonilla, L. Bougueleret, E. Boutet, L. Breuza, A. Bridge, R. Britto, H. Hye- A-Bye, C. Casals, E. Cibrian-Uhalte, E. Coudert, I. Cusin, P. Duek-Roggli, A. Estreicher, L. Famiglietti, P. Gane, P. Garmiri, G. Georghiou, A. Gos, N. Gruaz-Gumowski, E. Hatton-Ellis, U. Hinz, A. Holmes, C. Hulo, F. Jungo, G. Keller, K. Laiho, P. Lemercier, D. Lieberherr, A. Mac- Dougall, M. Magrane, M.J. Martin, P. Masson, D.A. Natale, C. O'Donovan, I. Pedruzzi, K. Pichler, D. Poggioli, S. Poux, C. Rivoire, B. Roechert, T. Sawford, M. Schneider, E. Speretta, A. Shypitsyna, A. Stutz, S. Sundaram, M. Tognolli, C. Wu, I. Xenarios, L.S. Yeh, J. Chan, S. Gao, K. Howe, R. Kishore, R. Lee, Y. Li, J. Lomax, H.M. Muller, D. Raciti, K. Van Auken, M. Berriman, L. Stein, Kersey Paul, P.W. Sternberg, D. Howe, M. Westerfield, Expansion of the gene ontology knowledgebase and resources: the gene ontology consortium, Nucleic Acids Res. 45 (2017) D331–D338, https://doi.org/10.1093/nar/gkw1108.
[30] M. Ashburner, C.A. Ball, J.A. Blake, D. Botstein, H. Butler, J.M. Cherry, A.P. Davis, K. Dolinski, S.S. Dwight, J.T. Eppig, M.A. Harris, D.P. Hill, L. Issel-Tarver, A. Kasarskis, S. Lewis, J.C. Matese, J.E. Richardson, M. Ringwald, G.M. Rubin, G. Sherlock, Gene ontology: tool for the unification of biology, Nat. Genet. 25 (2000) 25–29, https://doi.org/10.1038/75556.
[31] S. Iwano, M. Sugiyama, H. Hama, A. Watakabe, N. Hasegawa, T. Kuchimaru, K. Z. Tanaka, M. Takahashi, Y. Ishida, J. Hata, S. Shimozono, K. Namiki, T. Fukano, M. Kiyama, H. Okano, S. Kizaka-Kondoh, T.J. McHugh, T. Yamamori, H. Hioki, S. Maki, A. Miyawaki, Single-cell bioluminescence imaging of deep tissue in freely moving animals, Science 80 (359) (2018) 935–939, https://doi.org/10.1126/science.aaq1067.
[32] M. Nakano, M. Ito, R. Tanaka, H. Ariyama, K. Mitsugi, A. Makiyama, K. Uchino, T. Esaki, N. Tsuruta, F. Hanamura, K. Yamaguchi, Y. Okumura, K. Sagara, K. Takayoshi, K. Nio, K. Tsuchihashi, S. Tamura, H. Shimokawa, S. Arita, K. Miyawaki, H. Kusaba, K. Akashi, E. Baba, Epithelial-mesenchymal transition is activated in CD44-positive malignant ascites tumor cells of gastrointestinal cancer, Cancer Sci. 109 (2018) 3461–3470, https://doi.org/10.1111/cas.13777.
[33] H. Zhou, M. Sivasankar, D.H. Kraus, V.C. Sandulache, M. Amin, R.C. Branski, Glucocorticoids regulate extracellular matrix metabolism in human vocal fold fibroblasts, Laryngoscope 121 (2011) 1915–1919, https://doi.org/10.1002/lary.21920.
[34] S. Jaiswal, P. Fontanillas, J. Flannick, A. Manning, P. V Grauman, B.G. Mar, R. C. Lindsley, C.H. Mermel, N. Burtt, A. Chavez, J.M. Higgins, V. Moltchanov, F. C. Kuo, M.J. Kluk, B. Henderson, L. Kinnunen, H.A. Koistinen, C. Ladenvall, G. Getz, A. Correa, B.F. Banahan, S. Gabriel, S. Kathiresan, H.M. Stringham, M. I. McCarthy, M. Boehnke, J. Tuomilehto, C. Haiman, L. Groop, G. Atzmon, J. G. Wilson, D. Neuberg, D. Altshuler, B.L. Ebert, Age-related clonal hematopoiesis associated with adverse outcomes, N. Engl. J. Med. 371 (2014) 2488–2498, https://doi.org/10.1056/NEJMoa1408617.
[35] S. Jaiswal, P. Natarajan, A.J. Silver, C.J. Gibson, A.G. Bick, E. Shvartz, M. McConkey, N. Gupta, S. Gabriel, D. Ardissino, U. Baber, R. Mehran, V. Fuster, J. Danesh, P. Frossard, D. Saleheen, O. Melander, G.K. Sukhova, D. Neuberg, P. Libby, S. Kathiresan, B.L. Ebert, Clonal hematopoiesis and risk of atherosclerotic cardiovascular disease, N. Engl. J. Med. 377 (2017) 111–121, https://doi.org/10.1056/NEJMoa1701719.
[36] H.Y. Chang, J.-T.J. Chi, S. Dudoit, C. Bondre, M. van de Rijn, D. Botstein, P. O. Brown, M. Van De Rijn, D. Botstein, P.O. Brown, Diversity, topographic differentiation, and positional memory in human fibroblasts, Proc. Natl. Acad. Sci. Unit. States Am. 99 (2002) 12877–12882, https://doi.org/10.1073/pnas.162488599.
[37] J.H. Lee, T. Tammela, M. Hofree, J. Choi, N.D. Marjanovic, S. Han, D. Canner, K. Wu, M. Paschini, D.H. Bhang, T. Jacks, A. Regev, C.F. Kim, Anatomically and functionally distinct lung mesenchymal populations marked by Lgr5 and Lgr6, Cell 170 (2017) 1149–1163, https://doi.org/10.1016/j.cell.2017.07.028, e12.
[38] T.T. Braga, J.S.H. Agudelo, N.O.S. Camara, Macrophages during the fibrotic process: M2 as friend and foe, Front. Immunol. 6 (2015) 1–8, https://doi.org/10.3389/fimmu.2015.00602.
[39] H. Möllmann, H.M. Nef, S. Kostin, C. von Kalle, I. Pilz, M. Weber, J. Schaper, C. W. Hamm, A. Elsässer, Bone marrow-derived cells contribute to infarct remodelling, Cardiovasc. Res. 71 (2006) 661–671, https://doi.org/10.1016/j.cardiores.2006.06.013.
[40] S.J. Forbes, F.P. Russo, V. Rey, P. Burra, M. Rugge, N.A. Wright, M.R. Alison, A significant proportion of myofibroblasts are of bone marrow origin in human liver fibrosis, Gastroenterology 126 (2004) 955–963, https://doi.org/10.1053/j.gastro.2004.02.025.
[41] M. Quante, S.P. Tu, H. Tomita, T. Gonda, S.S.W. Wang, S. Takashi, G.H. Baik, W. Shibata, B. Diprete, K.S. Betz, R. Friedman, A. Varro, B. Tycko, T.C. Wang, Bone marrow-derived myofibroblasts contribute to the mesenchymal stem cell niche and promote tumor growth, Cancer Cell 19 (2011) 257–272, https://doi.org/10.1016/j.ccr.2011.01.020.
[42] A. Huijbers, R.A.E.M. Tollenaar, G.W. V Pelt, E.C.M. Zeestraten, S. Dutton, C. C. McConkey, E. Domingo, V.T.H.B.M. Smit, R. Midgley, B.F. Warren, E. C. Johnstone, D.J. Kerr, W.E. Mesker, The proportion of tumor-stroma as a strong prognosticator for stage II and III colon cancer patients: validation in the victor trial, Ann. Oncol. 24 (2013) 179–185, https://doi.org/10.1093/annonc/mds246.
[43] F. De Sousa E Melo, X. Wang, M. Jansen, E. Fessler, A. Trinh, L.P.M.H. de Rooij, J. H. de Jong, O.J. de Boer, R. van Leersum, M.F. Bijlsma, H. Rodermond, M. van der Heijden, C.J.M. van Noesel, J.B. Tuynman, E. Dekker, F. Markowetz, J.P. Medema, L. Vermeulen, Poor-prognosis colon cancer is defined by a molecularly distinct subtype and develops from serrated precursor lesions, Nat. Med. 19 (2013) 614–618, https://doi.org/10.1038/nm.3174.
[44] A. Sadanandam, C. a Lyssiotis, K. Homicsko, E. a Collisson, W.J. Gibb, S. Wullschleger, L.C.G. Ostos, W. a Lannon, C. Grotzinger, M. Del Rio, B. Lhermitte, A.B. Olshen, B. Wiedenmann, L.C. Cantley, J.W. Gray, D. Hanahan, A colorectal cancer classification system that associates cellular phenotype and responses to therapy, Nat. Med. 19 (2013) 619–625, https://doi.org/10.1038/nm.3175.
[45] L. Marisa, A. de Reyniès, A. Duval, J. Selves, M.P. Gaub, L. Vescovo, M.C. Etienne-Grimaldi, R. Schiappa, D. Guenot, M. Ayadi, S. Kirzin, M. Chazal, J.F. Fléjou, D. Benchimol, A. Berger, A. Lagarde, E. Pencreach, F. Piard, D. Elias, Y. Parc, S. Olschwang, G. Milano, P. Laurent-Puig, V. Boige, Gene expression classification of colon cancer into molecular subtypes: characterization, validation, and prognostic value, PLoS Med. 10 (2013), https://doi.org/10.1371/journal.pmed.1001453.
[46] A. Sadanandam, X. Wang, F. De Sousa E Melo, J.W. Gray, L. Vermeulen, D. Hanahan, J.P. Medema, Reconciliation of classification systems defining molecular subtypes of colorectal cancer: interrelationships and clinical implications, Cell Cycle 13 (2014) 353–357, https://doi.org/10.4161/cc.27769.
[47] C. Isella, A. Terrasi, S.E. Bellomo, C. Petti, G. Galatola, A. Muratore, A. Mellano, R. Senetta, A. Cassenti, C. Sonetto, G. Inghirami, L. Trusolino, Z. Fekete, M. De Ridder, P. Cassoni, G. Storme, A. Bertotti, E. Medico, Stromal contribution to the colorectal cancer transcriptome, Nat. Genet. 47 (2015) 312–319, https://doi.org/10.1038/ng.3224.
[48] S. Müller, G. Kohanbash, S.J. Liu, B. Alvarado, D. Carrera, A. Bhaduri, P. B. Watchmaker, G. Yagnik, E. Di Lullo, M. Malatesta, N.M. Amankulor, A. R. Kriegstein, D.A. Lim, M. Aghi, H. Okada, A. Diaz, Single-cell profiling of human gliomas reveals macrophage ontogeny as a basis for regional differences in macrophage activation in the tumor microenvironment, Genome Biol. 18 (2017) 234, https://doi.org/10.1186/s13059-017-1362-4.
[49] J.J. Fuster, S. MacLauchlan, M.A. Zuriaga, M.N. Polackal, A.C. Ostriker, R. Chakraborty, C. Wu, S. Sano, S. Muralidharan, C. Rius, J. Vuong, S. Jacob,

V. Muralidhar, A.A.B. Robertson, M.A. Cooper, V. Andrés, K.K. Hirschi, K. A. Martin, K. Walsh, Clonal hematopoiesis associated with TET2 deficiency accelerates atherosclerosis development in mice, Science 355 (2017) 842–847, https://doi.org/10.1126/science.aag1381.

[50] L. Helming, S. Gordon, Molecular mediators of macrophage fusion, Trends Cell Biol. 19 (2009) 514–522, https://doi.org/10.1016/j.tcb.2009.07.005.

[51] V.T. Fabris, A. Sahores, S.I. Vanzulli, L. Colombo, A.A. Molinolo, C. Lanari, C. A. Lamb, Inoculated mammary carcinoma-associated fibroblasts: contribution to hormone independent tumor growth, BMC Cancer 10 (2010), https://doi.org/10.1186/1471-2407-10-293.

[52] J. Linxweiler, T. Hajili, C. Körbel, C. Berchem, P. Zeuschner, A. Müller, M. Stöckle, M.D. Menger, K. Junker, M. Saar, Cancer-associated fibroblasts stimulate primary tumor growth and metastatic spread in an orthotopic prostate cancer xenograft model, Sci. Rep. 10 (2020) 1–13, https://doi.org/10.1038/s41598-020-69424-x.

[53] C.B. Nanthakumar, R.J.D. Hatley, S. Lemma, J. Gauldie, R.P. Marshall, S.J. F. Macdonald, Dissecting fibrosis: therapeutic insights from the small-molecule toolbox, Nat. Rev. Drug Discov. 14 (2015) 693–720, https://doi.org/10.1038/nrd4592.

[54] R.J. Akhurst, A. Hata, Targeting the TGFβ signalling pathway in disease, Nat. Rev. Drug Discov. 11 (2012) 790–811, https://doi.org/10.1038/nrd3810.

[55] S.A. Mani, W. Guo, M.-J. Liao, E.N. Eaton, A. Ayyanan, A.Y. Zhou, M. Brooks, F. Reinhard, C.C. Zhang, M. Shipitsin, L.L. Campbell, K. Polyak, C. Brisken, J. Yang, R.A. Weinberg, The epithelial-mesenchymal transition generates cells with properties of stem cells, Cell 133 (2008) 704–715, https://doi.org/10.1016/j.cell.2008.03.027.

[56] J. Rodon, M.A. Carducci, J.M. Sepulveda-Sánchez, A. Azaro, E. Calvo, J. Seoane, I. Braña, E. Sicart, I. Gueorguieva, A.L. Cleverly, N.S. Pillay, D. Desaiah, S. T. Estrem, L. Paz-Ares, M. Holdhoff, J. Blakeley, M.M. Lahn, J. Baselga, First-in-human dose study of the novel transforming growth factor-β receptor I kinase inhibitor LY2157299 monohydrate in patients with advanced cancer and glioma, Clin. Cancer Res. 21 (2015) 553–560, https://doi.org/10.1158/1078-0432.CCR-14-1380.

[57] G. Giaccone, L.A. Bazhenova, J. Nemunaitis, M. Tan, E. Juhász, R. Ramlau, M. M. van den Heuvel, R. Lal, G.H. Kloecker, K.D. Eaton, Q. Chu, D.J. Dunlop, M. Jain, E.B. Garon, C.S. Davis, E. Carrier, S.C. Moses, D.L. Shawler, H. Fakhrai, A phase III study of belagenpumatucel-L, an allogeneic tumour cell vaccine, as maintenance therapy for non-small cell lung cancer, Eur. J. Cancer 51 (2015) 2321–2329, https://doi.org/10.1016/j.ejca.2015.07.035.